Hindawi
Complexity
Volume 2022, Article ID 9663746, 11 pages
https://doi.org/10.1155/2022/9663746

Research Article

Design of a Small Quadruped Robot with Parallel Legs

Ming Lu, Baorui Jing, Hao Duan, and Guanbin Gao

Faculty of Mechanical and Electrical Engineering, Kunming University of Science and Technology, Kunming 650500, China

Correspondence should be addressed to Baorui Jing; jingbarry@163.com

Received 14 June 2022; Revised 13 September 2022; Accepted 15 September 2022; Published 29 September 2022

Academic Editor: Wenjie Lu

In this paper, a lightweight and modular design of a quadruped robot with two-degree-of-freedom parallel legs is presented. To reduce the weight and enhance the transmission accuracy, the horizontal layout of the driving end is adopted for designing the legs of the quadruped robot. The rotation angle of each actuator for the quadruped robot is analyzed by the inverse kinematics algorithm. Moreover, the trajectory of the foot-end, including support and swing phases, is planned to reduce the impact between the foot-end and the ground. Furthermore, the gait of the four legs of the quadruped robot is designed by considering the conditions of trot, standing, take-off, and walking. Finally, the effectiveness of the foot-end trajectory and the stable gait is verified by conducting experiments on a prototype platform.

1. Introduction

Mobile robots have become a research hotspot in the field of robotics since they can perform dangerous tasks in place of humans in rescue and disaster relief, anti-terrorist and explosive ordnance disposal, and field exploration [1]. Mobile robots can be divided into wheeled, crawler-type, and legged [2]. Although wheeled robots and crawler robots can move efficiently on relatively flat ground, they cannot work normally in cluttered terrains such as mountains and hills. In contrast, legged robots can overcome almost all terrain obstacles and have broader application prospects [3]. According to the number of feet, legged robots can be divided into biped robots, quadruped robots, and multi-legged robots. Among them, quadruped robots are currently receiving more attention because they have better stability and higher load capacity than biped robots, more flexible motion performance, and higher motion efficiency than multi-legged robots [4].

Over the past few decades, many excellent quadruped robots have been developed. Among them, the large-scale quadruped robots mainly include BigDog [5], LS3 [6], Wildcat [7], and HyQserial [8, 9]. These quadruped robots are hydraulically driven and more than 100 kg such that they can perform large-load rugged terrain traversal tasks. However, due to their large weight, large size, and power source (hydraulics) limitations, the main obstacle to the wider commercial utilization of large-scale quadruped robots is complicated. Of the medium-sized quadruped robots, the outstanding ones are MIT Cheetah [10–12], ANYmal [13, 14], Spot [15], and Aliengo [16]. By using motor-based proprioceptive actuators and electrically powered actuators, medium-sized quadruped robots have shown excellent motion performance. However, the development difficulty and the cost of hardware are too high to be suitable for widespread rollout [17–20]. Therefore, it is of great practical significance to develop a quadruped robot that is suitable for robot beginners, that can be used in home entertainment and school teaching scenarios.

In this paper, a small quadruped robot with parallel legs is designed. The leg structure adopts a parallel configuration with the horizontal layout of the driving end so that the leg actuator can meet the installation requirements of the steering engine and have the performance of low self-weight and high transmission accuracy. The body adopts a lightweight and modular design, which not only improves the motion performance but also has the characteristics of convenient disassembly and assembly. For the designed new leg parallel configuration, the corresponding forward and inverse kinematic algorithm is proposed. Through foot-end

trajectory planning and gait planning, it can obtain stable walking ability. The prototype uses an STM32 microcontroller as the main controller, and the steering engine as the actuator, and is assembled by using 3D printed mechanical structural parts. The experimental results verify that the quadruped robot designed in this paper not only has excellent motion performance but also has the advantages of low power consumption, small size, low cost, simple operation, etc. Therefore, it has certain entertainment, teaching, and practical value.

This paper is organized as follows: the second section introduces the mechanical structure design of this quadruped robot. In Section three, an inverse kinematics algorithm for the novel parallel leg configurations is proposed. The fourth and fifth sections, respectively, introduce the methods of foot-end trajectory planning and gait planning applied to this robot. The implementation scheme of the prototype and its experimental results are illustrated in Section six. Finally, the conclusion is given in Section seven.

2. Mechanical Structure Design of Quadruped Robot

Inspired by the bionic principle of quadrupeds, the mechanical structure of quadruped robots is generally designed as two parts: torso and limbs. Most of the limbs are designed as a three-degree-of-freedom serial mechanism [2], and the structure is distributed from bottom to top as foot-ankle-calf-knee-thigh-hip- torso, respectively. After some simplification, the quadruped robot based on the serial leg configuration can be obtained as shown in Figure 1.

However, there are some problems with such serial legs in practical applications. Firstly, due to the load accumulation effect of the serial mechanism [21], the joint actuator needs to bear the additional load of other parts of the leg; thus, the overall carrying capacity of the quadruped robot is limited, which appears to be overwhelmed in the case of weight-bearing tasks. In particular, it will cause great weight-bearing pressure on the knee joint, affecting the motion stability and the life of the actuator. Secondly, the actuators are usually installed at the knee joints of the legs in a serial configuration [3], which not only increases the moment of inertia of the legs but also increases the load on the hip joint actuators, making the robot action cumbersome and affecting the control effect. To solve this problem, one type of solution is to place the actuator of the knee joint at the hip joint and transmit power through a transmission mechanism such as a synchronous belt. However, the use of the transmission mechanism will introduce transmission errors. Coupled with the cumulative error of the serial mechanism itself, it is difficult to guarantee the accuracy of the foot-end, thus reducing the motion performance of the robot.

Due to the natural disadvantages of the serial configuration, the parallel configuration is more suitable for small quadruped robots with limited actuator output power [22]. A typical quadruped robot with a parallel leg configuration is the Stanford Doggo [23], which utilizes a coaxial parallel mechanism and a quasi-direct drive actuator to achieve excellent vertical jumping agility. However, the cost of the quasi-direct drive actuator is too high, and the control is difficult, so it is not suitable for large-scale promotion, and the supporting coaxial mechanism does not match the installation of the lower-cost steering engine.

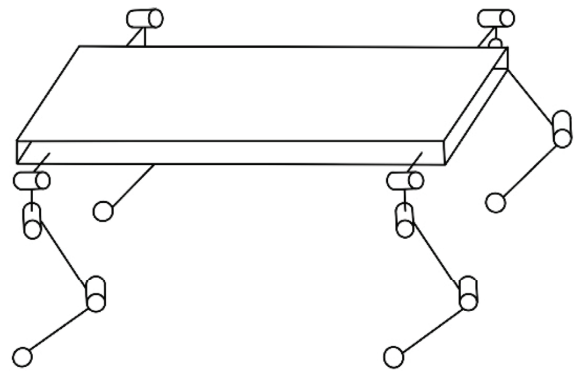

Figure 1: Quadruped robot based on serial leg configuration.

This paper refers to the parallel leg configuration of Stanford Doggo, splits the coaxial mechanism and arranges the actuators horizontally, and designs a 2-DOF parallel leg mechanism as shown in Figure 2. The mechanism has two active joints (hip joints) driven by steering engines, which are mounted horizontally at A and E on the side of the torso, and these two steering engines together control the movement of one leg. B, C, and D are passive joints without a power source, wherein B and D are the knee joints, and C is the foot end. The knee joints B and D change the position of the foot-end C with the rotation of the hip joints A and E.

The mechanism has the following advantages: First, the actuator can be installed in the torso to protect the actuator and reduce the moment of inertia of the legs. Second, the parallel leg mechanism has less transmission error and therefore has higher control accuracy. Compared with the 3-DOF series mechanism, this solution reduces the space and self-weight and increases the load capacity due to the subtraction of one hip joint transverse swing degree of freedom. In addition, the steering function responsible for the hip joint can be replaced by the differential method. Compared to the Stanford Doggo, our quadruped robot uses a small, low-cost steering engine as the actuator, eliminating the need for a separate gearbox and allowing the two actuators to be mounted horizontally with a direct drive output, thereby reducing the overall size of the robot and simplifying the structure.

Figure 3 illustrates the structure of the quadruped robot. The torso adopts a lightweight and modular design. It is 3D printed with PLA material, and the shape of which is a rectangular parallelepiped with four edges cut off, where the head and tail ends are connected by hollow brackets. This design can minimize weight reduction while maintaining strength, thereby improving athletic performance. The centre of the torso is the control module, which is used to place the controller and battery compartment, and its top is equipped with a boat-shaped power switch and a hinged battery compartment opening and closing cover for easy start-up and battery replacement. Eight steering engines are drive modules, which are symmetrically installed on both sides of the front and rear parts of the torso and extend out of

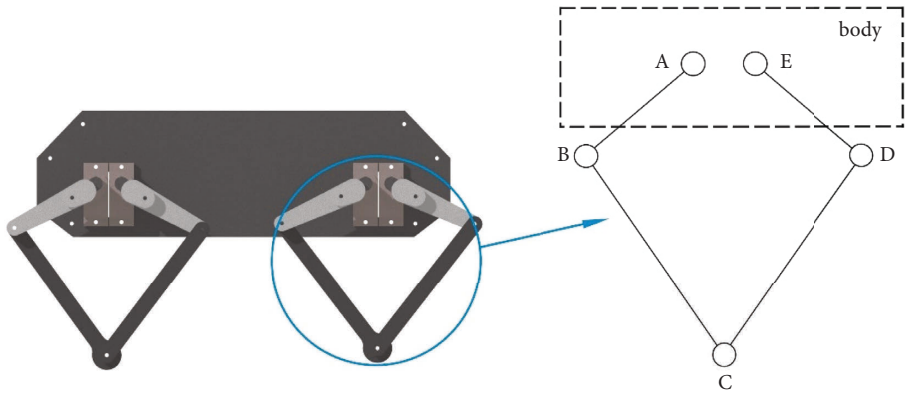

Figure 2: The 2-DOF parallel leg mechanism.

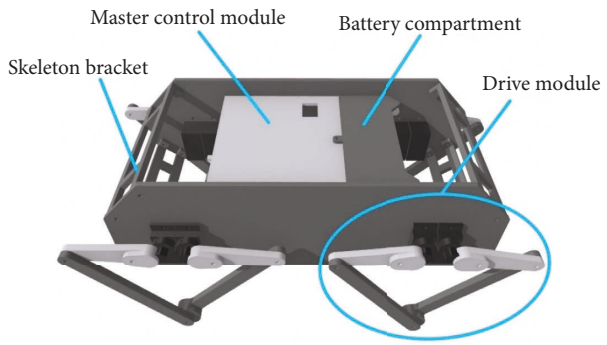

Figure 3: Small quadruped robot with a parallel leg mechanism.

the output shaft to connect the parallel leg mechanism. This layout makes the centre of gravity coincide with the centroid, ensuring control stability. Meanwhile, the modular design gives the quadruped robot the characteristics of quick assembly and easy replacement of parts.

The front and top views of the quadruped robot are shown in Figures 4 and 5, respectively, and its structural design parameters are listed in Table 1.

3. Kinematic Analysis of Legs

Kinematic analysis refers to the analysis of position, velocity, and acceleration changes of the mechanism without considering the force action, respectively. These three change analyses are also the pivot between the active input components and the passive output components of the mechanism. In this section, the forward and inverse kinematic analysis of the legs of the quadruped robot designed in this paper is performed separately.

By modeling the parallel leg mechanism, a Cartesian base coordinate system is established with the straight line where the two hip joints are located as the x-axis and the midpoint of the two hip joints as the origin, and the schematic diagram of the joint coordinates can be obtained as in Figure 6. Wherein, the definitions of joints A, B, C, D, and E are the same as in Figure 2, which make up a five-bar linkage. Define the lengths of AE, AB, DE, BC, and CD as l, l_1, l_1, l_2, l_2. The angles between each link and the x-axis are denoted as θ_1, θ_2, θ_3, θ_4 (range from 0 to 180 degrees) as shown in Figure 2. Moreover, the coordinate of the foot-end point C is represented by (x, y).

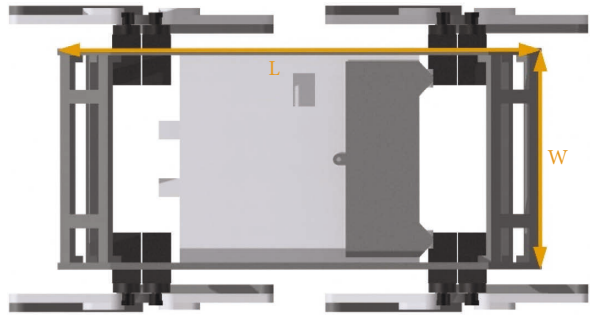

Figure 4: Top view of the quadruped robot.

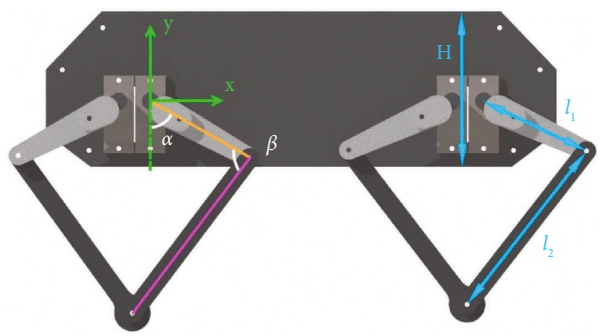

Figure 5: Side view of the quadruped robot.

Table 1: The structural design parameters.

Symbol	Description	Value
W	Torso width	96 mm
L	Torso length	210 mm
H	Torso high	64 mm
l	Interval of motor	15 mm
l_1	Length of thigh	50 mm
l_2	Length of calf	80 mm
α	Hip joint rotation range	−90°~+90°
β	Knee joint rotation range	15°~175°
M	Total mass	0.44 kg

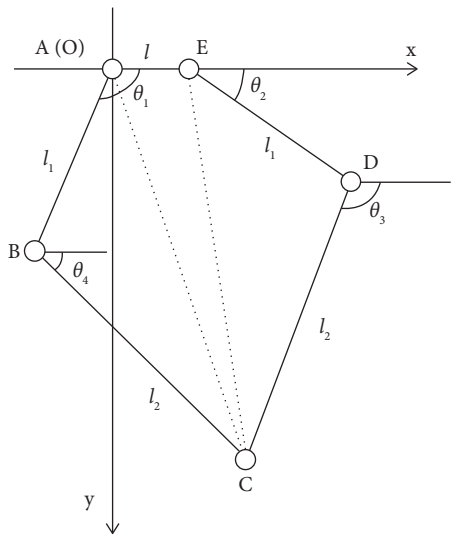

Figure 6: The schematic diagram of joint coordinates of parallel leg mechanism.

First, the matrix method is used for forwarding kinematics analysis. Calculating the projection lengths in the x and y directions, respectively, we can obtain the system of equations as

$$\begin{cases} l + l_1 \cos\theta_2 + l_2 \cos\theta_3 = l_2 \cos\theta_4 + l_1 \cos\theta_1, \\ l_1 \sin\theta_2 + l_2 \sin\theta_3 = l_2 \sin\theta_4 + l_1 \sin\theta_1. \end{cases} \tag{1}$$

According to Table 1, we have known the exact values of l, l_1 and l_2. In addition, the angles of θ_1 and θ_2 are active joints, thus the unknown variables are θ_3 and θ_4. By placing the unknown variable to the left of the equal sign, (1) becomes

$$\begin{cases} l_2 \cos\theta_3 - l_2 \cos\theta_4 = l_1 \cos\theta_1 - l_1 \cos\theta_2 - l, \\ l_2 \sin\theta_3 - l_2 \sin\theta_4 = l_1 \sin\theta_1 - l_1 \sin\theta_2. \end{cases} \tag{2}$$

Solving (2) by computer software, e.g., MATLAB, we can calculate the value of joints θ_3 and θ_4. Thereby, the coordinate of the foot-end point C can be solved as

$$\begin{aligned} &x\text{: } l + l_1 \cos\theta_2 + l_2 \cos\theta_3 \text{ or } l_2 \cos\theta_4 + l_1 \cos\theta_1, \\ &y\text{: } l_1 \sin\theta_2 + l_2 \sin\theta_3 \text{ or } l_2 \sin\theta_4 + l_1 \sin\theta_1. \end{aligned} \tag{3}$$

The relationship of joint angular velocity can be obtained by calculating the first derivative of (2) with respect to time as

$$l_2 \begin{bmatrix} -\sin\theta_3 & \sin\theta_4 \\ \cos\theta_3 & -\cos\theta_4 \end{bmatrix} \begin{bmatrix} \omega_3 \\ \omega_4 \end{bmatrix} = l_1 \begin{bmatrix} -\sin\theta_1 & \sin\theta_2 \\ \cos\theta_1 & -\cos\theta_2 \end{bmatrix} \begin{bmatrix} \omega_1 \\ \omega_2 \end{bmatrix}, \tag{4}$$

where the symbols $\omega_1 \sim \omega_4$ are the angular velocities of $\theta_1 \sim \theta_4$.

Based on the velocity function (4), the accelerate function can be further derived as

$$\begin{aligned} l_2 \begin{bmatrix} -\sin\theta_3 & \sin\theta_4 \\ \cos\theta_3 & -\cos\theta_4 \end{bmatrix} \begin{bmatrix} \alpha_3 \\ \alpha_4 \end{bmatrix} = &-l_2 \begin{bmatrix} -\omega_3 \cos\theta_3 & \omega_4 \cos\theta_4 \\ -\omega_3 \sin\theta_3 & \omega_4 \sin\theta_4 \end{bmatrix} \begin{bmatrix} \omega_3 \\ \omega_4 \end{bmatrix} + l_1 \begin{bmatrix} -\sin\theta_1 & \sin\theta_2 \\ \cos\theta_1 & -\cos\theta_2 \end{bmatrix} \begin{bmatrix} \alpha_1 \\ \alpha_2 \end{bmatrix} \\ &+ l_1 \begin{bmatrix} -\omega_1 \cos\theta_1 & \omega_2 \cos\theta_2 \\ -\omega_1 \sin\theta_1 & \omega_2 \sin\theta_2 \end{bmatrix} \begin{bmatrix} \omega_1 \\ \omega_2 \end{bmatrix}, \end{aligned} \tag{5}$$

where, the symbols $\alpha_1 \sim \alpha_4$ are the angular accelerations of $\theta_1 \sim \theta_4$. Therefore, by solving functions (4) and (5), we can obtain the angular velocities ω_3, ω_4 and the angular accelerations α_3, α_4.

Then, the inverse kinematic analysis of the legs is also conducted. The so-called inverse kinematics is to find the rotation angle of each actuator with the knowledge of the coordinates of the foot-end relative to the leg base coordinate system. Using the inverse kinematics algorithm, the mapping relationship between the position of the foot-end and the angles of the actuators can be determined, thus achieving the purpose of foot-end position control. In this section, the inverse kinematics analysis is performed for the novel parallel leg mechanism designed in this paper to obtain the leg inverse kinematics algorithm applicable to our quadruped robot. According to the algebraic method, the angle of each joint is solved as follows:

$$l_{AC} = \sqrt{x^2 + y^2}, \tag{6}$$

$$l_{EC} = \sqrt{(x - l)^2 + y^2}. \tag{7}$$

Then according to the cosine theorem, we can infer the value of $\angle CAE$, $\angle CEA$, $\angle BAC$, $\angle CED$, namely,

$$\begin{aligned} \angle CAE &= \cos^{-1} \frac{l^2 + l_{AC}^2 - l_{EC}^2}{4 l_{AC} l}, \\ \angle CEA &= \cos^{-1} \frac{l^2 + l_{EC}^2 - l_{AC}^2}{4 l_{EC} l}, \\ \angle BAC &= \cos^{-1} \frac{l_1^2 + l_{AC}^2 - l_2^2}{2 l_1 l_{AC}}, \\ \angle CED &= \cos^{-1} \frac{l_1^2 + l_{EC}^2 - l_2^2}{2 l_1 l_{EC}}. \end{aligned} \tag{8}$$

$$\angle CED = \cos^{-1} \frac{l_1^2 + l_{EC}^2 - l_2^2}{2 l_1 l_{EC}}. \tag{9}$$

Finally, by combining (7), (9), we can derive θ_1 and θ_2 as:

$$\theta_1 = \angle CAE + \angle BAC, \tag{10}$$

$$\theta_2 = \pi - \angle CEA - \angle CED. \tag{11}$$

Equations (10)~(11) are the inverse kinematics algorithm of the novel parallel leg mechanism designed in this paper.

4. Trajectory Planning of Foot-End

Although the inverse kinematics solution can be used in positioning control for the foot-end of the quadruped robot, to make the foot-end move according to the preset trajectory, it is necessary to plan a reasonably foot-end trajectory. The planned trajectory can be discrete into a sequence of foot-end trajectory points to be sent to the controller, thereby achieving foot-end trajectory control.

To illustrate the trajectory of the foot-end, we need first to introduce some concepts as follows [24].

(i) Gait Cycle: The duration of the robot's leg from the moment it hits the ground to the next moment it hits the ground, represented by T_s

(ii) Support Phase: The state when one leg is supported on the ground

(iii) Swing Phase: The state when one leg is off the ground

(iv) Duty Ratio: The ratio of the time occupied by the swing phase of one leg to the whole gait cycle

It was found that the cycloid trajectory can reduce the impact of the foot landing so that the quadruped robot has better stability in motion. Therefore, this paper adopts the cycloid method to plan the foot-end trajectory. By setting the gait parameters of the quadruped robot such as the step length, step height, and cycle, the foot trajectory is obtained as

$$\begin{cases} x_{\exp} = \left(x_f - x_s\right)\dfrac{\sigma - \sin\sigma}{2\pi} + x_s, \\ y_{\exp} = h\dfrac{1 - \cos\sigma}{2} + y_s, \end{cases} \tag{12}$$

where $(x_{\exp}, y_{\exp})$ is the coordinates of the desired foot-end point, (x_s, y_s) is the coordinate of the foot-end starting point, h is the step height, which is the maximum height of the foot-end from the ground, $x_f - x_s$ is the step size, i.e., the distance between the landing point x_f and the starting point x_s. parameter $\sigma = 2\pi t/\lambda T_s$, where $0 < t < T_s$, T_s the cycle time of the whole foot-end trajectory, λ is the duty ratio of the swing phase.

The whole trajectory is divided into the support phase and swing phase, the duty ratio of the swing phase in the whole cycle time T_s can be adjusted by the duty ratio parameter λ. Also, the cycle time T_s, the step height h, and the step size $x_f - x_s$ can be changed according to different environments and speed requirements. For example, when $\lambda = 0.5$, $T_s = 1s$, $h = 10mm$ and $x_f - x_s = 20mm$, the trajectory and speed curve of the foot-end are depicted in Figures 7 and 8.

Through the analysis of the speed curve of the foot-end (Figure 8), it can be seen that the speed curve of the robot remains continuous in one motion cycle, and the velocity in the x-direction and y-direction is zero at the moment when the foot-end touches the ground and leaves the ground, which can effectively reduce the impact between the foot-end and the ground and helps to maintain the motion stability of the quadruped robot.

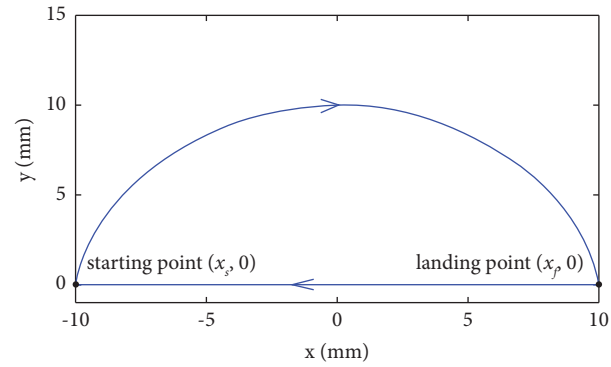

Figure 7: The cycloid trajectory of foot-end.

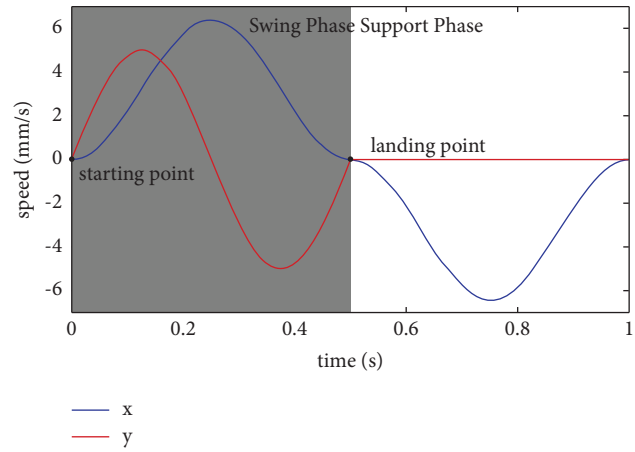

Figure 8: The speed curve of the foot-end.

5. Gait Planning

The foot-end trajectory only specifies the action of one leg. To make the quadruped robot move, it is necessary to reasonably distribute the action rhythm of the four legs, that is, gait planning. In bionics, gait refers to the movement pattern of a footed animal, that is, the fixed positional relationship between the individual legs. The quadruped robot designed in this paper adopts the mainstream trot gait and walking gait to obtain the corresponding behavioral capabilities. To describe gait, the four legs are labeled in Figure 9, where RF, LF, LH, and RH represent the right front leg, the left front leg, the left hind leg, and the right hind leg.

The trotting gait is suitable for the fast walking of the quadruped robot, which means that the two legs on the diagonal move in the same way. Currently, the legs on the two diagonals move in the opposite direction, and the support phase and the swing phase of the foot-end trajectory of one leg each account for half of the cycle time. Figure 10 displays the timing diagram of the trot gait, where a couple

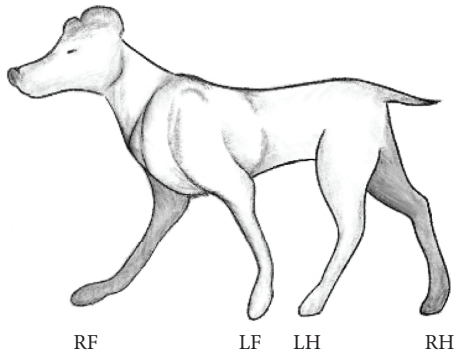

Figure 9: The label has four legs.

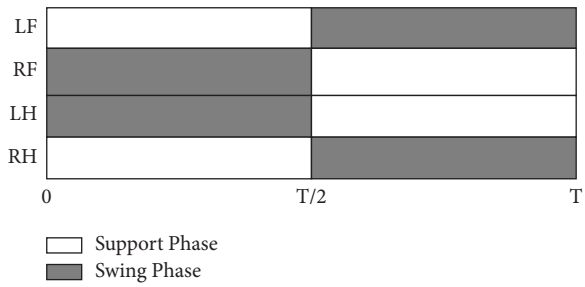

Figure 10: The timing diagram of the trot gait.

of legs in one diagonal are in the state of support phase while another couple of legs are in the state of swing phase. Since the trot gait has high energy efficiency, it can be adapted to a large speed range [24]. Furthermore, this kind of symmetrical gait is also conducive to maintaining the stability of quadruped robots and has become the most used gait for quadruped robots.

The differential steering gait is the most common gait used for the steering of an 8-DOF quadruped robot. Based on the trot gait, the differential steering gait changes the foot-end step length or the leg swing direction on both sides of the robot, where a displacement difference is generated to rotate the robot body.

The walking gait is also a widely used gait, which is suitable for the slow walking of quadruped robots. When a quadruped robot is performing the walking gait, there are always three legs on the ground. At this time, the support phase of each leg occupies 3/4 of the cycle, and the swing phase occupies 1/4 of the cycle. The positions of the four legs in a cycle are different from each other, differing by 1/4 of a cycle in turn, as shown in Figure 11.

6. Prototype and Experiments

The prototype uses SolidWorks software to design the mechanical structure, and the mechanical parts are produced by 3D printing. The control system of the prototype is shown in Figure 12, in which the controller is the STM32f103c8t6 minimum core board, and the control program is written through Keil software. The actuator used in the quadruped robot is the mg90s steering engine, which is driven by the PCA9685 driver board. In terms of power supply, a 7.4 V rechargeable lithium battery is used to power the control system and steering engine after it is stepped down to 5 V by the LM2596 step-down module. The control system is also equipped with a PS2 signal receiver, which is responsible for receiving the remote-control signal from the PS2 handle. The major functions of the controller STM32 are calculation and communication. The calculation function is responsible for planning the gait of the robot and executing the inverse kinematics solution. The communication function is in charge of communicating with the PS2 receiver and the PCA9685 driver board.

By receiving the remote-control signal from the PS2 handle, STM32 transmits the calculated motor position signal to the PCA9685 driver board to realize the motion control. The rotation angle of the steering engine is controlled by the PWM signal, which is output through PCA9685. Note that the corresponding relationships between the rotation angle and the PWM signal are illustrated in Figure 13.

It can be seen from Figure 13 that the rotation angle can be controlled by adjusting the duty cycle of the PWM signal. Note that the duty cycle refers to the proportion of high-level duration in one signal period. Then, according to the relationship, we can calculate the duty cycle ω as

$$\omega = \frac{0.5 + (\varphi/180) \times (2.5 - 0.5)}{20}, \tag{13}$$

where φ is the rotation angle of the steering engine.

By using (13), we can achieve angle control of a steering engine by sending PWM signals from the controller to the driver board.

Figure 14 is the picture of the prototype. It has been verified by experiments that the prototype can perform the trot gait and walk gait well. In addition, based on the trot gait, the in-situ stepping gait, the in-situ take-off gait, and the lateral gait relying on the offset of the centre of gravity are developed.

Compared with similar quadruped robots, the design cost of our robot is extremely low. Table 2 lists the cost of each component required to build the robot.

We conducted experiments on the motion of the robot's legs on a motion capture system (Figure 15). In this experiment, four calibration balls were installed on one leg of the robot, and the robot was controlled to walk forward, then the foot-end trajectory of the robot in the world coordinate system could then be obtained. Use Matlab to draw the velocity curve of the trajectory as shown in Figure 16. Compared with Figure 8, the actual speed curve obtained in the experiment is consistent with the design curve, and it can be clearly seen that the swing phase and the support phase account for half of each gait cycle.

To evaluate the performance of our quadruped robot, we introduce the concept of "Normalized Work Capability" (NWC) [25]. NWC represents the proportional relationship between Normalized Speed (NS) and Payload Capacity (PLC). Where NS is the ratio of maximum speed to body length, reflecting the performance of speed per unit body

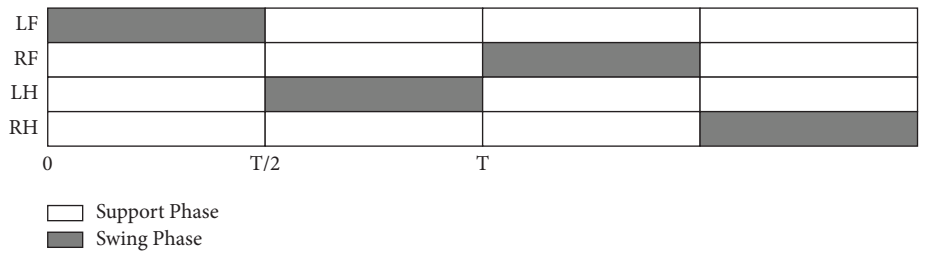

Figure 11: The timing diagram of the walking gait.

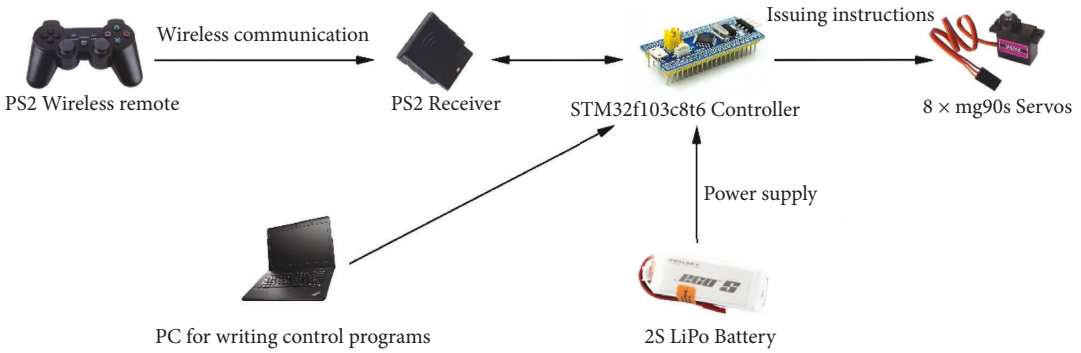

Figure 12: The control system of the prototype.

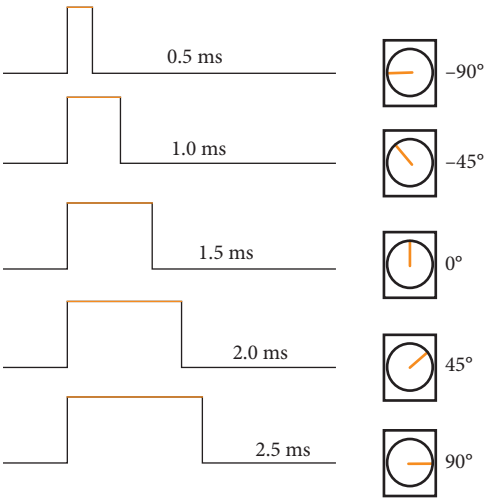

Figure 13: The corresponding relationship between the rotation angle and the PWM signal.

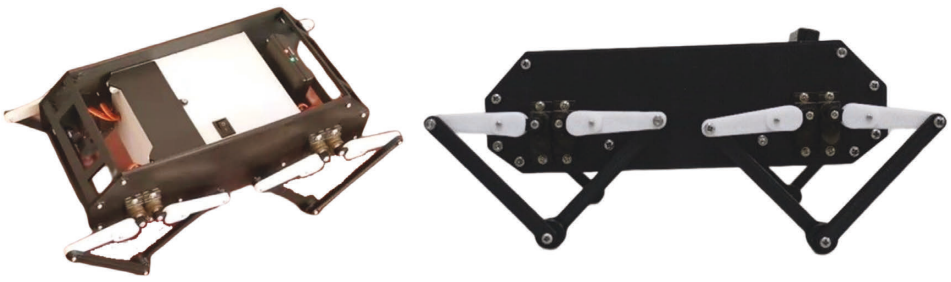

Figure 14: The prototype.

Table 2: The prototype BOM.

Item	Price	Quantity	Cost
MG90S steering engines	6.85	8	54.80
3D print parts	53.00 (RMB/kg)	0.21 (kg)	11.13
STM32f103c8t6 controller	36.88	1	36.88
PCA9685 driver board	23.00	1	23.00
2S 800 mAh lithium battery	26.13	1	26.13
PS2 handle	45.00	1	45.00
LM2596 step-down module	3.60	1	3.6
		Total:	200.54 RMB

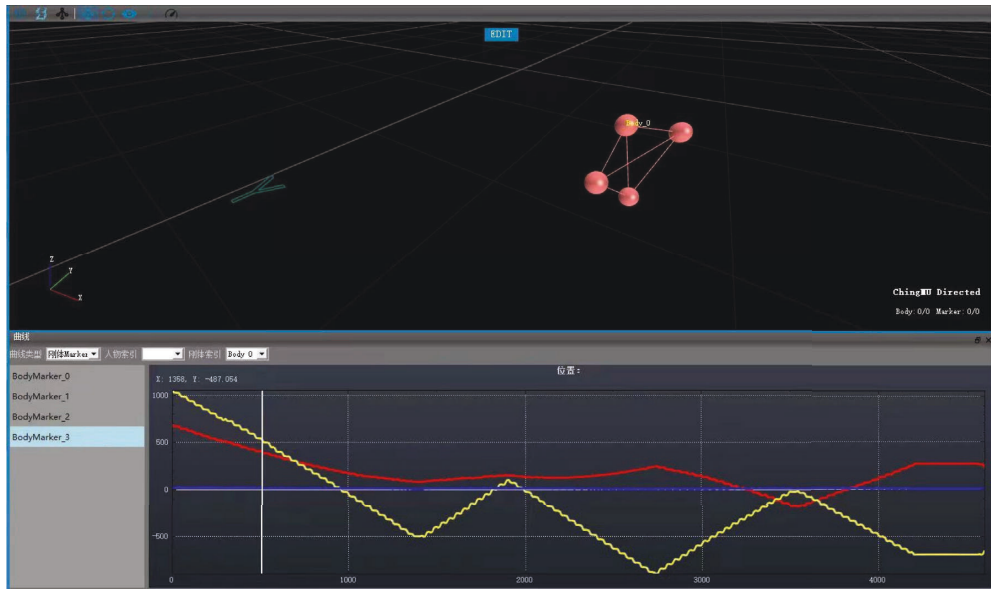

Figure 15: The experiment in the motion capture system.

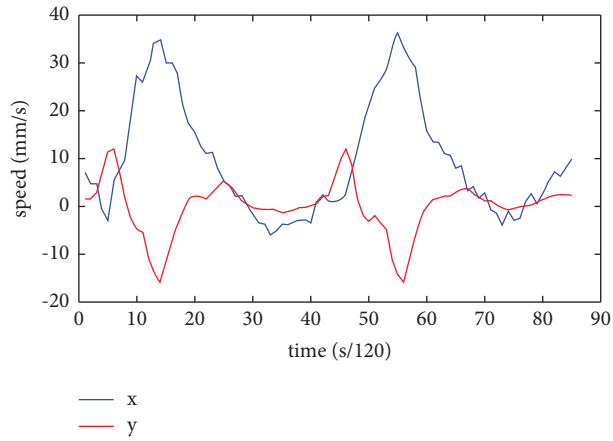

Figure 16: The actual speed curves.

length, the greater the value, the better. The PLC refers to the ratio of the robot's weight to the payload, reflecting the required self-weight per unit load, the smaller the value, the better. Therefore, NWC is the integrated performance of NS and PLC. The larger the value, the better. For the small parallel-legged quadruped robot designed in this paper, the NS, PLC, and NWC are 1.36%, 55.31%, and 75.22%, respectively. Compared with the data of other famous quadruped robots provided in reference [3], we can conclude that the performance of the mechanical dog designed in this paper is at roughly average level [3]. The comparison results are shown in Figures 17~19. Because the new

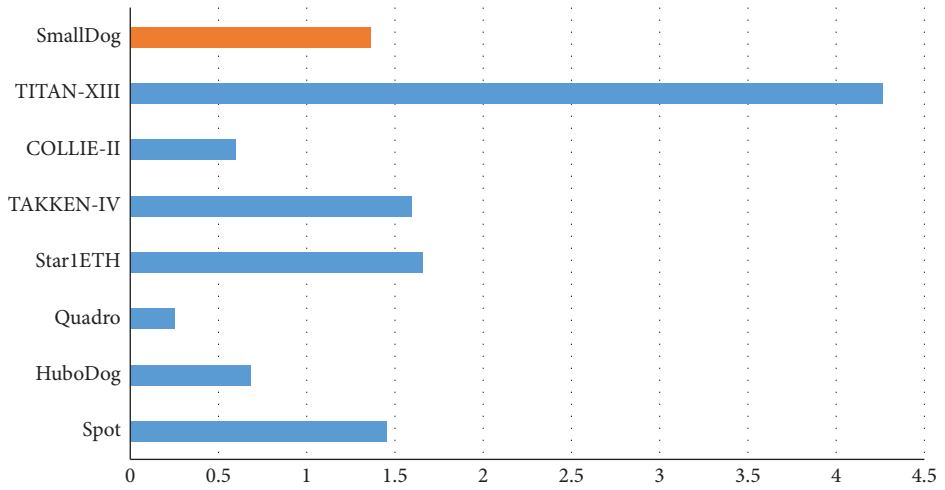

Figure 17: Normalized speed.

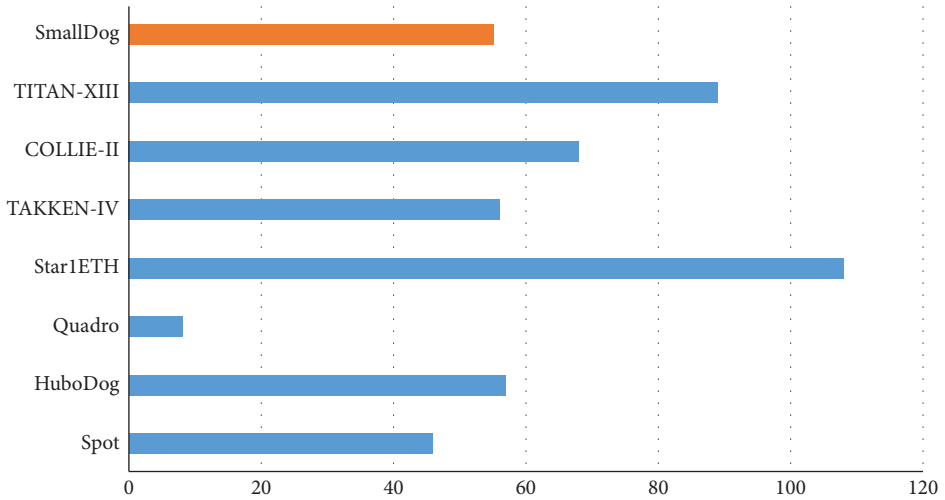

Figure 18: Payload capacity.

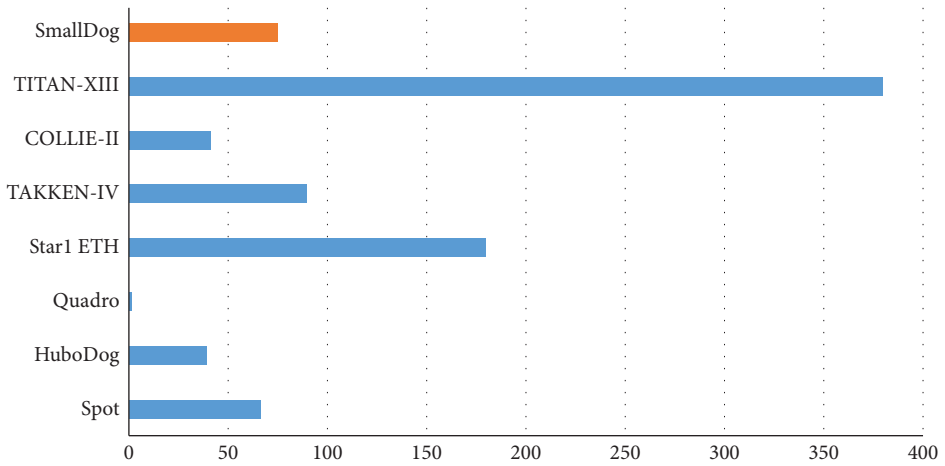

Figure 19: Normalized work capacity.

quadruped robot has lower cost and thus higher cost performance, it is more suitable for promotion to the entertainment and teaching market.

7. Conclusion

In this paper, a small, low-cost, and simple-to-operate two-degree-of-freedom parallel leg configuration is designed and realized. Besides, the structure, kinematics analyses, foot trajectory, and gait planning of the designed quadruped robot are studied. First, from the perspective of bionics and mechanics, this paper adopts the parallel scheme of the horizontal layout of the driving end and the concepts of lightweight and modularization and designs a quadruped robot with low self-weight, simple structure, and high transmission performance. In the quadruped robot structure, the actuator is installed in the fuselage, which protects the actuator and reduces the moment of inertia of the legs. Second, the paper analyses the two-degree-of-freedom parallel leg configuration. By using the matrix method, we performed a kinematic analysis of the legs and used the inverse kinematics algorithm to determine the mapping relationship between the position of the foot end of each leg and the angle of the leg actuator, to achieve the purpose of position control. Furthermore, the paper verifies the effectiveness of the cycloid trajectory and the stability of the mainstream gait by planning the trajectory and gait of the quadruped robot. Finally, this paper builds a quadruped whole machine experiment platform with two degrees of freedom in parallel leg configuration and conducts related experiments on trot gait and walking gait. Based on the trot gait, the experiment extended the gait in situ, gait in- situ jumping, and lateral movement gait relying on the offset of the centre of gravity, which verifies the correctness of the prototype design method and control algorithm. Compared with commercial products, the mechanical dog designed in this paper is made by 3D printing, so the structure of the legs can be arbitrarily changed, and the corresponding kinematics algorithm can also be adapted to the modifications by adjusting the parameters of the legs. In addition, the controller is completely open source so that any desired functionality can be added. Based on the above advantages, people can customize a mechanical dog that is different in structure and program on the basis of the prototype, thus meeting the needs of teaching and entertainment. Moreover, the cost of this robot has been compressed to 200 RMB, and its performance is no less than that of other well-known quadruped robots, which greatly reduces the development threshold of quadruped robots.

Data Availability

Data were curated by the authors and are available upon request.

Conflicts of Interest

The authors declare that there are no conflicts of interest regarding the publication of this paper.

Acknowledgments

This work was supported by the National Natural Science Foundation of China (Grant no. 51865020).

References

[1] L. Yao, H. Yu, and Z. Lu, "Design and driving model for the quadruped robot: an elucidating draft," *Advances in Mechanical Engineering*, vol. 13, no. 4, 2021.

[2] X. Meng, S. Wang, Z. Cao, and L. Zhang, "A review of quadruped robots and environment perception," in *Proceedings of the 2016 35th Chinese Control Conference (CCC)*, pp. 6350–6356, Chengdu, China, July 2016.

[3] P. Biswal and P. K. Mohanty, "Development of quadruped walking robots: a review," *Ain Shams Engineering Journal*, vol. 12, no. 2, pp. 2017–2031, 2021.

[4] D. J. Todd, *Walking Machines: An Introduction to Legged Robots*, Springer Science & Business Media, Germany, 2013.

[5] M. Raibert, K. Blankespoor, G. Nelson, and R. Playter, "BigDog, the rough-terrain quadruped robot," *IFAC Proceedings Volumes*, vol. 41, no. 2, pp. 10822–10825, 2008.

[6] B. Dynamics, "LS3 - Legged Squad Support System," 2012, https://www.youtube.com/watch?v=R7ezXBEBE6U.

[7] "Boston Dynamics, Introducing WildCat," 2013, https://www.youtube.com/watch?v=wE3fmFTtP9g.

[8] C. Semini, V. Barasuol, J. Goldsmith et al., "Design of the hydraulically actuated, torque-controlled quadruped robot HyQ2Max," *IEEE*, vol. 22, no. 2, pp. 635–646, 2017.

[9] C. Semini, N. G. Tsagarakis, E. Guglielmino, M. Focchi, F. Cannella, and D. G. Caldwell, "Design of HyQ – a hydraulically and electrically actuated quadruped robot," *Proceedings of the Institution of Mechanical Engineers - Part I: Journal of Systems & Control Engineering*, vol. 225, no. 6, pp. 831–849, 2011.

[10] G. Bledt, M. J. Powell, B. Katz, J. Di Carlo, P. M. Wensing, and S. Kim, "MIT Cheetah 3: Design and Control of a Robust, Dynamic Quadruped Robot," in *Proceedings of the 2018 IEEE/RSJ International Conference on Intelligent Robots and Systems (IROS)*, pp. 2245–2252, Madrid, Spain, October 2018.

[11] P. M. Wensing, A. Wang, S. Seok, D. Otten, J. Lang, and S. Kim, "Proprioceptive actuator design in the MIT Cheetah: impact mitigation and high-bandwidth physical interaction for dynamic legged robots," *IEEE Transactions on Robotics*, vol. 33, no. 3, pp. 509–522, 2017.

[12] S. Seok, A. Wang, M. Y. Chuah, D. Otten, J. Lang, and S. Kim, "Design Principles for Highly Efficient Quadrupeds and Implementation on the MIT Cheetah Robot," in *Proceedings of the 2013 IEEE International Conference on Robotics and Automation*, pp. 3307–3312, Karlsruhe, Germany, May 2013.

[13] P. Fankhauser and M. Hutter, "ANYmal: A Unique Quadruped Robot Conquering Harsh Environments," *Research Features*, vol. 126, pp. 54–57, 2018.

[14] M. Hutter, C. Gehring, D. Jud et al., "ANYmal - a Highly mobile and Dynamic Quadrupedal Robot," in *Proceedings of the 2016 IEEE/RSJ International Conference on Intelligent Robots and Systems (IROS)*, pp. 38–44, Daejeon, Korea, October 2016.

[15] *Spot® - the Agile Mobile Robot*, Boston Dynamics, Waltham, Massachusetts, USA, 2022.

[16] Z. Chen, "Aliengo—versatility and industry applications," *Unitree*, https://www.unitree.com/aliengo/, 2022.

[17] S. Xie and Q. Chen, "Adaptive nonsingular predefined-time control for attitude stabilization of rigid spacecrafts," *IEEE Transactions on Circuits and Systems II: Express Briefs*, vol. 69, no. 1, pp. 189–193, 2022.

[18] M. Tao, Q. Chen, X. He, and S. Xie, "Fixed-time filtered adaptive parameter estimation and attitude control for quadrotor UAVs," *IEEE Transactions on Aerospace and Electronic Systems*, p. 1, 2022.

[19] D. Xiao, H. Chen, C. Wei, and X. Bai, "Statistical measure for risk-seeking stochastic wind power offering strategies in electricity markets," *J. Mod. Power Syst. Clean Energy*, 2021.

[20] C. Wei, Y. Zhao, Y. Zheng, L. Xie, and K. Smedley, "Analysis and Design of a Non-isolated High Step-Down Converter with Coupled Inductor and ZVS Operation," *IEEE Trans. Ind. Electron*, vol. 69, pp. 9007–9018, 2021.

[21] K.-H. Grote and E. K. Antonsson, *Springer handbook of mechanical engineering*, Vol. 10, Springer, Berlin, Germany, 2009.

[22] L. Li, Y. Fang, S. Guo, H. Qu, and L. Wang, "Type synthesis of a class of novel 3-DOF single-loop parallel leg mechanisms for walking robots," *Mechanism and Machine Theory*, vol. 145, Article ID 103695, 2020.

[23] N. Kau, A. Schultz, N. Ferrante, and P. Slade, "Stanford Doggo: An Open-Source, Quasi-Direct-Drive Quadruped," 2019, http://arxiv.org/abs/1905.04254.

[24] A. Spröwitz, A. Tuleu, M. Vespignani, M. Ajallooeian, E. Badri, and A. J. Ijspeert, "Towards dynamic trot gait locomotion: design, control, and experiments with Cheetah-cub, a compliant quadruped robot," *The International Journal of Robotics Research*, vol. 32, no. 8, pp. 932–950, 2013.

[25] M. B. Binnard, *Design of a Small Pneumatic Walking Robot*, Massachusetts Institute of Technology, Cambridge, Massachusetts, USA, 1995.